

PACS numbers: 42.25.Lc; 42.55.Rz
DOI: 10.1070/QE2003v033n10ABEH002516

Compensation for thermally induced birefringence in polycrystalline ceramic active elements

M.A. Kagan, E.A. Khazanov

***Abstract*. Polycrystalline ceramics differ significantly from single crystals in that the crystallographic axes (and, hence, the axes of thermally induced birefringence) are oriented randomly in each grain of the ceramic. The quaternion formalism is employed to calculate the depolarisation in the ceramics and the efficiency of its compensation. The obtained analytic expressions are in good agreement with the numerical relations. It is shown that the larger the ratio of the sample length to the grain size, the closer the properties of the ceramics to those of a single crystal with the [111] orientation (in particular, the uncompensated depolarisation is inversely proportional to this ratio).**

Keywords: *Nd* : *YAG ceramics, thermally induced depolarisation, birefringence*.

1. Introduction

In recent years, considerable attention has been paid to the problem of using polycrystalline Nd : YAG ceramics (see Refs [1 – 6] and references therein) and other cubic crystals [7] as active media. This attention stems from the considerable advantage that ceramics have over single crystals. Modern technology can be used for preparing ceramic active elements (AEs) with good optical quality, large aperture and a high concentration of the neodymium ions. Many properties of ceramics are close to those of a single crystal, but a number of differences are observed in the thermally induced depolarisation of radiation in the two cases [6].

A polycrystalline ceramics consists of a large number of monocrystalline grains of size 10 – 100 μm separated by thin ($\sim$ 1 nm) boundaries. A significant distinction between such ceramics and a single crystal is that the crystallographic axes in each grain are oriented randomly. Like a single crystal, the ceramics is also isotropic. Moreover, in the absence of thermal effects, the ceramics is almost free from depolarisation [2]. The photoelastic effect associated with a temperature gradient leads to birefringence in single crystals as well as ceramics. In contrast to a single crystal, however, the ceramics is a system of phase plates with randomly oriented axes and a random phase delay between eigen polarisations. The analytic expressions for eigen polarisations and phase delays between them were derived in Ref. [6].

The aim of our paper is to derive analytic expressions for depolarisation of radiation caused by thermally induced birefringence, and to study the efficiency of compensation for depolarisation by the methods employed for single crystals. Instead of the conventional Jones matrix formalism, we used the quaternion formalism [8, 9], according to which each grain has a normalised quaternion (hypercomplex number) associated with it.

2. Eigen polarisations and phase delays between them in ceramics

Consider a cylindrical ceramic AE of radius R_0 and length L. We shall calculate depolarisation in the geometrical optics approximation, i.e., treat the wave packet incident on the sample as a bundle of beams parallel to the sample axis z. Figure 1 shows one such beam passing at a distance r from the sample axis and having an azimuthal angle φ.

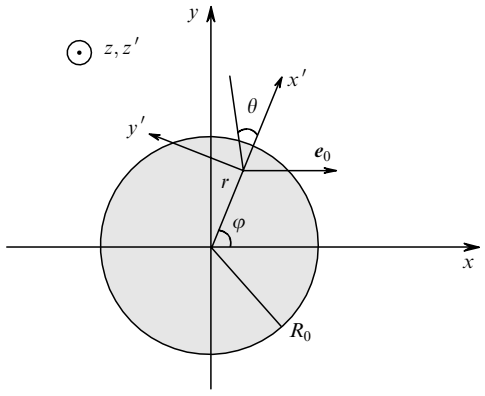

Figure 1. Mutual arrangement of the coordinate systems xyz and $x'y'z'$.

Suppose that the power densities of heat release in an AE and heat sink are independent of z and φ. The radially symmetric temperature gradient defines two preferred directions, radial and azimuthal, in each cross section $z = \text{const}$. The eigen polarisations may not coincide with these directions since the polarisation properties of each grain depend on thermoelastic stresses (which, in turn,

M.A. Kagan, E.A. Khazanov Institute of Applied Physics, Russian Academy of Sciences, ul. Ul'yanova 46, 603950 Nizhnii Novgorod, Russia; e-mail: kagmic@mail.nnov.ru; khazanov@appl.sci-nnov.ru

Received 17 October 2002; revision received 20 January 2003
Kvantovaya Elektronika **33** (10) 876 – 882 (2003)
Translated by Ram Wadhwa

depend on photoelastic coefficients) determined by the temperature distribution and orientation of the coordinate system of the crystallographic axes *abc* relative to the laboratory reference frame *xyz* [6, 10]. In the simplest case, the axes *abc* coincide with the axes *xyz*, which corresponds to the [001] orientation.

An arbitrary orientation of the axes *abc* can be set with the help of three successive rotations of the coordinate system *xyz* by the Euler angles α, β and Φ relative to the crystal lattice [11]. At first, the coordinate system is turned through an angle α ($\alpha \in [-\pi, \pi]$) around the z axis coinciding with the c axis, after which it is turned around the y axis through an angle β ($\beta \in [-\pi/2, \pi/2]$) and, finally, once again about the z axis through an angle Φ ($\Phi \in [-\pi, \pi]$). Thus, the orientation of the crystal axes *abc* in each grain is determined by three angles, viz., α, β and Φ which are random quantities distributed uniformly over the corresponding intervals. Since the system does not have gyrotropy or dichroism, each grain can be treated from the polarisation point of view as a linear phase plate characterised by two random quantities, i.e., the angle θ of inclination of eigen polarisations (relative to the x' axis), and the phase difference δ between them. Consequently, a ceramic sample is equivalent to a sequence of such phase plates.

Using the expressions presented in Ref. [6], we arrive at the following relations connecting θ and δ with the Euler angles α, β and Φ for each grain:

$$\tan 2\theta = \frac{\tilde{b}}{\tilde{a}}, \quad \delta = -\frac{p}{N}\frac{l_g}{\langle l_g \rangle}\frac{\tilde{a}}{\cos 2\theta}, \tag{1}$$

where

$$\tilde{a} = 2\xi h + \frac{\xi - 1}{4}(g\sigma_1 + h\tau_1); \quad \tilde{b} = \frac{\xi - 1}{4}(g\sigma_2 + h\tau_2); \tag{2}$$

$$\sigma_1 = \sin^2\beta\{[8\cos^2\beta - \sin^2 2\alpha(3 + \cos 2\beta)]\cos 2\Phi' + 2\cos\beta \sin 4\alpha \sin 2\Phi'\};$$

$$\sigma_2 = \sin^2\beta\{[8\cos^2\beta - \sin^2 2\alpha(3 + \cos 2\beta)]\sin 2\Phi' - 2\cos\beta \sin 4\alpha \cos 2\Phi'\};$$

$$\tau_1 = -4\cos^2\beta - \sin^4\beta(4 - \sin^2\alpha) - \cos 4\Phi' \times [\sin^4\beta(4 - \sin^2 2\alpha) + 4\cos^2\beta\cos 4\alpha] - \sin 4\Phi' \sin 4\alpha \cos\beta(3 + \cos 2\beta);$$

$$\tau_2 = \sin 4\alpha \cos\beta(3 + \cos 2\beta)\cos 4\Phi' - [\sin^4\beta(4 - \sin^2 2\alpha) + 4\cos^2\beta\cos 4\alpha]\sin 4\Phi';$$

$$p = \frac{P_h}{\lambda}\frac{a_T}{\kappa}\frac{n_0^3}{8}\frac{1 + v}{1 - v}(p_{11} - p_{12}); \quad \xi = \frac{2p_{44}}{p_{11} - p_{12}}; \quad \Phi' = \Phi - \varphi;$$

N is the number of grains; P_h is the power of heat release over the entire AE; λ is the wavelength; κ is the thermal conductivity; α_T is the coefficient of thermal expansion; n_0 is the refractive index without heating; v is the Poisson ratio; p_{ij} is the photoelastic coefficient; and l_g is the length of the grain (a normally distributed random quantity with a mean value $\langle l_g \rangle$ and a standard deviation σ_{len}). For fixed Euler angles, formulas (1) and (2) lead to the values of θ and δ for a single crystal with the corresponding orientation. For example, for [001] ($\alpha = \beta = \Phi = 0$) and [111] orientations ($\alpha = \pi/4$, $\tan\beta = \sqrt{2}$, Φ), we arrive at the following familiar relations [12]: $\tan(2\theta + 2\varphi) = \xi\tan 2\varphi$ and $\theta = 0$ respectively. Note that since Φ is a random quantity distributed uniformly over the interval $[-\pi, \pi]$, the prime over Φ in the expressions for $\sigma_{1,2}$ and $\tau_{1,2}$ can be disregarded for all averagings.

We shall restrict ourselves to the case of uniform heat release over the volume, for which

$$h = u/2, \quad g = u - 1/2, \tag{3}$$

where $u = (r/R_0)^2$. In the general case, the expressions for g and h are presented in Ref. [6]. Note that the quantityξ is a constant characterising the crystal. For example $\xi = 3.2$ for a Nd : YAG crystal.

It follows from (1) and (2) that the angle θ averaged over l_g, α, β and Φ is equal to zero. In the following analysis, we shall assume that random quantities l_g, α, β and Φ are independent for different grains. In other words, the distribution function F is assumed to be the product of distribution functions $f_i(l_g, \alpha, \beta, \Phi)$ for individual grains:

$$F(f_1, f_2, ..., f_N) = \prod_{i=1}^{N} f_i(l_g, \alpha, \beta, \Phi). \tag{4}$$

3. Depolarisation of radiation

Let a transverse electromagnetic wave be incident on an optical system without absorption, having the corresponding Jones matrix $\hat{U}$ connecting the polarisation $\boldsymbol{e}$ at the outlet of the system with its initial polarisation $\boldsymbol{e}_0$:

$$\boldsymbol{e} = \hat{U}\boldsymbol{e}_0 \quad (|\boldsymbol{e}| = |\boldsymbol{e}_0| = 1). \tag{5}$$

The local depolarisation Γ is defined as the fraction of the output power radiation corresponding to the polarisation $\boldsymbol{e}_\perp$, orthogonal to $\boldsymbol{e}_0$:

$$\Gamma = |\boldsymbol{e}_\perp^* \boldsymbol{e}|^2 = \boldsymbol{e}_0^* \hat{U}^* \boldsymbol{e}_\perp \boldsymbol{e}_\perp^* \hat{U}\boldsymbol{e}_0. \tag{6}$$

Hereafter, the asterisk indicates the Hermitian conjugate. Since the matrix $\hat{U}$ depends on r and φ, so does Γ. We shall find the depolarisation $\Gamma(r, \varphi)$ under the assumption that the incident beam was linearly polarised along the x axis, i.e., in the primed coordinate system (see Fig. 1)

$$\boldsymbol{e}_0 = \begin{pmatrix} \cos\varphi \\ -\sin\varphi \end{pmatrix}, \quad \boldsymbol{e}_0^* = (\cos\varphi, -\sin\varphi),$$
$$\boldsymbol{e}_\perp = \begin{pmatrix} \sin\varphi \\ \cos\varphi \end{pmatrix}, \quad \boldsymbol{e}_\perp^* = (\sin\varphi, \cos\varphi). \tag{7}$$

Formula (6) can be rewritten in the form

$$\Gamma = \boldsymbol{e}_0^* \hat{G}\boldsymbol{e}_0, \tag{8}$$

the matrix $\hat{G}$ is connected with the Jones matrix $\hat{U}$ through the relation

$$\hat{G} = \hat{U}^* \hat{M} \hat{U}, \tag{9}$$

where

$$\hat{M} = \begin{pmatrix} \sin^2\varphi & \sin\varphi\cos\varphi \\ \sin\varphi\cos\varphi & \cos^2\varphi \end{pmatrix}.$$

If the matrix $\hat{U}$ describes an optical system containing a ceramic element, it depends on random quantities l_{gi}, α_i, β_i, Φ_i, where i is the grain number. We denote by $\langle\hat{G}\rangle$ the matrix $\hat{G}$ averaged over all grains taking into account the distribution function (4). In this case, we obtain from (8) the following expression for average depolarisation:

$$\langle\Gamma\rangle = \boldsymbol{e}_0^* \langle\hat{G}\rangle \boldsymbol{e}_0. \tag{10}$$

The most interesting quantity is the integral depolarisation over the cross section:

$$\gamma = \frac{1}{\pi R_0^2}\int_0^{2\pi} \mathrm{d}\varphi \int_0^{R_0} \langle\Gamma\rangle(r,\varphi) r\mathrm{d}r = \frac{1}{2\pi}\int_0^{2\pi} \mathrm{d}\varphi \int_0^1 \langle\Gamma\rangle(u,\varphi)\mathrm{d}u. \tag{11}$$

Here and below, we shall assume that the beam intensity has the form

$$I = \begin{cases} I_0 & \text{for } r \leqslant R_0, \\ 0 & \text{for } r > R_0. \end{cases}$$

4. Compensation for depolarisation in various schemes

Let us calculate the average depolarisation in a ceramic AE, as well as in some schemes used for its compensation (Fig. 2). Depolarisation in ceramic elements without compensation (Fig. 2a) and in all schemes with compensation (Fig. 2b–d) is defined by expressions (10) and (11), the only difference being in the matrices $\hat{U}$ and $\hat{G}$ describing the optical system.

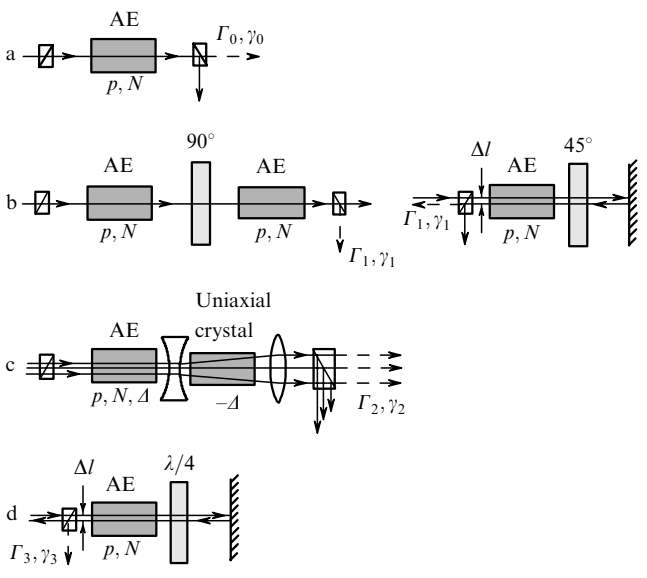

Figure 2. Measurements of the depolarisation (a) in an AE without compensation, (b) in scheme I with two AE and a 90°-rotator (left) [13] or with one AE and a Faraday mirror (right), (c) in scheme II with an AE and a uniaxial crystal [15], and (d) in scheme III with an AE and a $\lambda/4$ plate [16].

The Jones matrix $\hat{T}$ of a ceramic element is the product of Jones matrices of N phase plates corresponding to N grains:

$$\hat{T} = \hat{Q}_N \hat{Q}_{N-1} \ldots \hat{Q}_2 \hat{Q}_1, \tag{12}$$

where $\hat{Q}_k = \hat{Q}(\delta_k, \theta_k)$ is the matrix for the kth grain, and

$$\hat{Q}(\delta,\theta) = \begin{pmatrix} \cos\frac{\delta}{2} + \mathrm{i}\sin\frac{\delta}{2}\cos 2\theta & \mathrm{i}\sin\frac{\delta}{2}\sin 2\theta \\ \mathrm{i}\sin\frac{\delta}{2}\sin 2\theta & \cos\frac{\delta}{2} - \mathrm{i}\sin\frac{\delta}{2}\cos 2\theta \end{pmatrix}. \tag{13}$$

For the scheme without compensation (Fig. 2a), we obtain from (9) and (12) the matrix $\hat{G}_0$:

$$\hat{G}_0 = \hat{T}^* \hat{M} \hat{T} = \hat{Q}_1^* \hat{Q}_2^* \ldots \hat{Q}_{N-1}^* \hat{Q}_N^* \hat{M} \hat{Q}_N \hat{Q}_{N-1} \ldots \hat{Q}_2 \hat{Q}_1. \tag{14}$$

In order to calculate the matrix $\hat{G}$ corresponding to scheme I (Fig. 2b, left) [13], we denote by $\hat{T}_1$ and $\hat{T}_2$ the Jones matrices for the first and second AE respectively. In the absence of thermal effects in scheme I, the radiation emerging at the output will be polarised along the y axis, although the initial polarisation was directed along the x axis. Hence, for the sake of convenience in computations, we insert another $-90°$-rotator (not shown in Fig. 2b) after the second sample and calculate depolarisation as the fraction of power in the y-component of the field, i.e., in the component whose polarisation is orthogonal to the initial polarisation. In this case, $\hat{U}_\mathrm{I} = \hat{J}^* \hat{T}_2 \hat{J} \hat{T}_1 = \hat{T}_2^* \hat{T}_1$, where $\hat{J}$ is the 90°-rotation matrix and the matrix $\hat{T}_1$ is defined by the expression (12). Thus, the expression for $\hat{G}_1$ has the form

$$\hat{G}_1 = \hat{T}_1^* \hat{T}_2 \hat{M} \hat{T}_2^* \hat{T}_1. \tag{15}$$

In scheme I with a Faraday mirror [14] (Fig. 2b, right) two different ways are possible. If all the beams in their return path pass through the same grains as in the forward path, the depolarisation $\gamma \equiv 0$. On the contrary, if the transverse displacement Δl of a beam between direct and return paths is larger than, or of the order of, the grain size $\langle l_\mathrm{g}\rangle$, i.e., if the beam passes through different grains on its return trip, this scheme is completely equivalent to the scheme with a 90°-rotator (Fig. 2b, left).

The key element in scheme II (Fig. 2c) is a uniaxial crystal cut along the optical axis and mounted inside a telescope [15]. This crystal is described by the Jones matrix $\hat{Q}(-\Delta, 0)$ since its eigen linear polarisations are oriented along the azimuth and the radius. Consequently,

$$\hat{G}_2 = \hat{T}^* \hat{Q}(\Delta, 0) \hat{M} \hat{Q}(-\Delta, 0) \hat{T}, \tag{16}$$

where Δ is the effective phase delay in the ceramic [see formula (21)].

The axis of the $\lambda/4$ plate in scheme III (Fig. 2d) is parallel to the x axis [16]. A return trip through the $\lambda/4$ plate in the system of coordinates $x'y'$ is described by the Jones matrix $\hat{Q}(\pi, -\varphi)$. It follows hence that

$$\hat{G}_3 = \hat{T}_1^* \hat{Q}(-\pi, -\varphi) \hat{T}_2^* \hat{M} \hat{T}_2 \hat{Q}(\pi, -\varphi) \hat{T}_1. \tag{17}$$

Here, we assume that the beam passes through different grains on its return passage.

The mechanism of averaging formulas (14)–(17) over all grains for the case when their number is fixed and equal to N is described in the Appendix, where the expressions for $\langle \Gamma_{0-3} \rangle$ are also obtained. Substitution of these expressions into (11) gives

$$\gamma_0 = \frac{1}{4}\left(1 - \frac{\sin pX}{pX}\right) + \frac{p^2}{8N}\int_0^1 \left[\left(A + \frac{1}{2}B\right)\cos \Delta + B\right] du$$

$$- \frac{p}{16N}\int_0^1 \frac{B}{a}\sin \Delta \, du, \tag{18}$$

$$\gamma_1 = \frac{p^2}{4N}\int_0^1 \left(A + \frac{3}{2}B\right) du - \frac{p}{16N}\int_0^1 \frac{B}{a}\sin 2\Delta \, du, \ \gamma_2 = \frac{\gamma_1}{2}, \tag{19}$$

$$\gamma_3 = \frac{1}{4}\left(1 - \frac{\sin pX}{pX}\right) - \frac{1}{16}\left(1 - \frac{\sin 2pX}{2pX}\right)$$

$$+ \frac{p^2}{16N}\int_0^1 \{B[4\cos^2(\Delta/2) + 3\cos \Delta]$$

$$+ 2A[2 + \cos \Delta - \cos^2(\Delta/2)]\} du$$

$$- \frac{p^2}{32N}\int_0^1 \frac{B}{a}(\sin 2\Delta - \sin \Delta) \, du, \tag{20}$$

where

$$a = \langle \tilde{a} \rangle = 2Xh; \quad X = \frac{75\xi + 53}{128}; \quad \Delta = pa;$$

$$A = \langle \tilde{a}^2 \rangle - a^2 = (1 + d^2)\frac{h^2}{2^{14}}$$

$$\times (22665\xi^2 + 31470\xi + 11401) + B - 4(Xh)2; \tag{21}$$

$$B = \langle \tilde{b}^2 \rangle = (1 + d^2)\frac{(\xi - 1)^2}{2^{15}}(1060g^2 + 9865h^2); \quad d = \frac{\sigma_{\text{len}}}{\langle l_g \rangle}.$$

Note that this computational technique can considerably simplify the solution of problems on propagation of light in birefringence fibres with random inhomogeneities [17].

5. Discussion of results

It can be easily shown that if the ratio of the length of an AE to the average grain size tends to infinity ($N \to \infty$), then expressions (18)–(20) for γ_{0-3} are almost identical to the analogous expressions for a single crystal with the [111] orientation, the only difference being in the value of X which is $(1 + 2\xi)/3$, for a single crystal and $X = (75\xi + 53)/128$ or ceramics. In other words, for $N \to \infty$, the ceramics is equivalent to a single crystal with the [111] orientation and an effective constant ξ_{eff} defined by the expression

$$\xi_{\text{eff}} - 1 = (\xi - 1)(15/16)^2. \tag{22}$$

For example, $\xi = 3.2$, $\xi_{\text{eff}} = 2.9$ for the Nd : YAG ceramics. This leads to quite insignificant discrepancies in the integral depolarisations, which is in agreement with the experimental data [2].

Figures 3 and 4 show the dependence of depolarisation γ on the normalised radiation power p for an Nd : YAG ceramics in different schemes (curves) as well as the results of numerical computations based on the technique described in Ref. [6] (points). One can see that for a large value N of the ratio of the length of the AE to the average grain size, the numerical and analytic results have a nearly ideal matching.

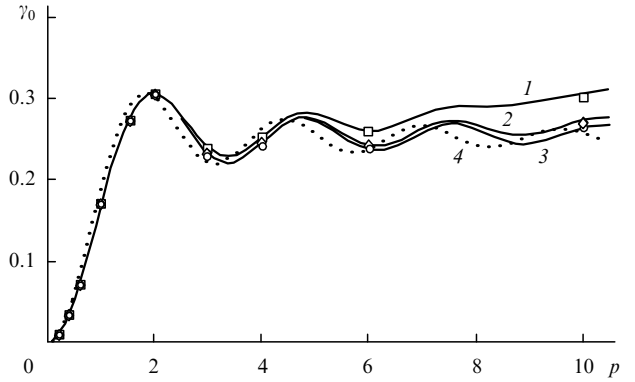

Figure 3. Dependences $\gamma_0(p)$ for ceramics for $N = 30$ (□, curve *1*), 100 (◇, curve *2*) and 300 (○, curve *3*), as well as for a single crystal (curve *4*).

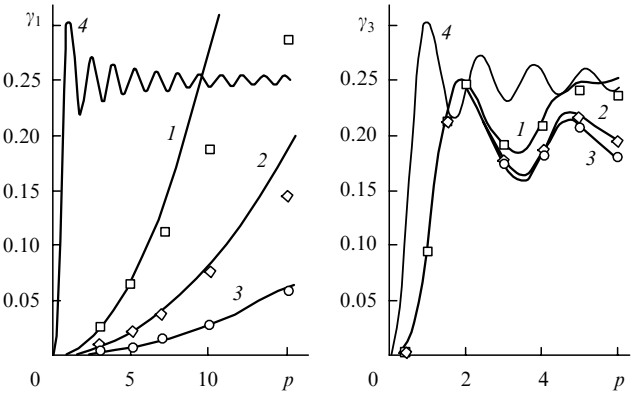

Figure 4. Dependences $\gamma_1(p)$ and $\gamma_3(p)$ for $N = 30$ (□, curve *1*), 100 (◇, curve *2*) and 300 (○, curve *3*). For comparison, curve (*4*) shows depolarisation in the absence of a 90°-rotator in scheme I and a $\lambda/4$ plate in scheme III.

Note that the length of the AE may vary from 2–3 mm in the case of diode pump to 10 cm for flashlamp pump, while the grain size may vary from 10 to 100 μm. Thus, the ratio N may change over a wide range from 20 to 1000. For an Nd : YAG ceramics, the expression for p can be presented in the form $p = 0.025P_{\text{h}}$. The power of heat release P_{h} may be as high as several hundred watts, and hence the parameter p varies from zero right up to 20. However, such an extent of heat release may destroy the sample.

For a single crystal, the depolarisation in schemes shown in Figs 2b and c is theoretically ideal, but the compensation for large heat release power is at the level 1 %–3 % in actual practice. If the parameters p and N are such that depolarisation is much smaller than this quantity, it can be assumed from the practical point of view that depolarisation in the ceramics does not exceed depolarisation in a single crystal with the [111] orientation.

For finite values of N, formulas (18)–(20) are obtained by expanding the expressions for depolarisation into a Taylor series in the small parameter $\varepsilon = p/N$ (see Appendix) if terms of the order of ε^2 are disregarded. This explains the disparity between the analytic and numerical results shown in Fig. 4 for quite large values of ε. Additional depolarisation (relative to the case $N = \infty$) is proportional to the square of the normalised radiation power p and is inversely proportional to N. This is due to dispersion of the local depolarisation D_Γ. Using an approach analogous to the one proposed in the Appendix, one can show that

$$D_\Gamma = (\langle \Gamma^2 \rangle - \langle \Gamma \rangle^2) \sim p^2/N, \tag{23}$$

which is also in accord with the numerical results [6] and is an important consequence of the random nature of birefringence in ceramics.

Indeed, consider an optical system formed by m successive ceramic samples, each of which is characterised by the number of grains N_0 and heat release power p_0. In this case, the system can be treated as a single sample containing $N = mN_0$ grains and corresponding to the power $p = mp_0$. According to (23), the dispersion of local depolarisation D_Γ in this system of elements will be m times higher than that in each individual sample ($D_{\Gamma 0}$), i.e., $D_\Gamma = mD_{\Gamma 0}$. The obtained results coincide with the classical problem of random walk in which the mean square displacement is proportional to the number of steps. Using the same arguments, we can explain the fact that $\gamma_2 = \gamma_1/2$ since only one ceramic AE is present in scheme II, while there are two such elements in scheme I.

All the constraints of compensation techniques known for a single crystal (e.g., the presence of a thick lens with a focal length commensurate with the length of the AE) are also applicable to ceramics. Beams separated in the transverse direction by a distance equal to the grain size pass through an independent set of grains, and will therefore have different values of depolarisation. Thus, a large-scale polar structure of polarised (and depolarised) output radiation will contain intensity modulation with a characteristic scale of the order of $\langle l_g \rangle$. This modulation is due to the dispersion of depolarisation D_Γ, the modulation depth increasing in proportion to the square of the normalised radiation power p and inversely proportional to the ratio N of the length of the AE to the average grain size. In addition to the above-mentioned amplitude modulation, phase modulation may also occur on account of the presence of grains of different sizes in the path of adjacent beams.

Consider the applicability of the geometrical approach used here. The size of a grain is much smaller than the characteristic scale of temperature gradient that determines the variation of the refractive index. Since the separation between grains (cavity size) is much smaller than the wavelength [2], it can be assumed that beams passing through ceramics will have nearly the same trajectory as the beams passing through a single crystal (curved on account of the thermal lens). A formula was obtained in Ref. [18] for mean-square lateral displacement of a beam ρ during the propagation of light in a randomly inhomogeneous medium. When applied to ceramics, this formula gives $\rho \approx 0.2N^{1/2}\lambda\pi$. As a rule, ρ is smaller than the average grain size $\langle l_g \rangle$. In the opposite case, the characteristic size of the above-mentioned modulation will be equal to ρ and not to $\langle l_g \rangle$.

Note also that the numerical results (points in Figs 3 and 4) were obtained by solving another more 'physical' problem in which the length of the AE is assumed to be fixed rather than the number N of grains [6]. These two formulations of the problem are exactly identical if we assume that the grain size l_g is fixed, which is the same as equating to zero the dispersion of the grain length $d = \sigma_{\text{len}}/\langle l_g \rangle = 0$ The dependences shown in Figs 3 and 4 are constructed just for this case. A comparison of the results obtained in these two cases is justified if $d < 1/N^{1/2}$. This condition means that the mean square deviation of the number of grains over the length of the sample does not exceed one, i.e., the number of grains in the sample can be assumed to be fixed. Note that the numerical computations reveal a weak dependence of depolarisation on the dispersion d of the grain size.

Polycrystalline ceramics can be used not only as an active medium and a Q-switch [19], but also for making Faraday isolators based on magnetoactive elements made of terbium gallium garnet (TGG). There are no fundamental difficulties in the path of creating TGG ceramics [20]. The above analysis can also be used for high average power Faraday isolators taking into account the specific character of depolarisation due to the imposition of a magnetic field [10].

6. Conclusions

The results of the paper can be summarised as follows:

1. If the ratio of the length of the AE to the average grain size tends to infinity, the polarisation properties of the ceramics are quite similar to those of a single crystal with the [111] orientation. In this case, the depolarisation dispersion tends to zero, while the depolarisation itself can be described for all schemes shown in Fig. 2 by the formulas for a single crystal with the [111] orientation taking into account the variation of the crystal parameter ξ as described by formula (22).

2. The efficiency of birefringence compensation by using standard techniques is worse in the ceramics than in a single crystal. The increase in depolarisation in the ceramics compared to a single crystal is proportional to the square of the normalised radiation power p and inversely proportional to the ratio N of the length of the AE to the average grain size.

3. Apart from the large-scale structure, both polarised and depolarised radiation also contain a random small-scale modulation with a characteristic transverse size equal to the grain size $\langle l_g \rangle$, and a depth proportional to p^2 and inversely proportional to N.

Appendix

Consider the method of averaging of expressions (14)–(17). This procedure is considerably simplified if, instead of the Jones formalism, we use the quaternion formalism (see Refs [8, 9] and the references cited therein) according to which each grain is decribed by a normalised quaternion (hypercomplex number). We shall first describe the transition from matrix representation to quaternion representation. Each optical element has a corresponding unitary Jones matrix $\hat{U}$ for which

$$\hat{U}\hat{U}^* = \hat{\sigma}_0 = \begin{pmatrix} 1 & 0 \\ 0 & 1 \end{pmatrix}, \tag{A1}$$

where the asterisk indicates Hermitian conjugation. An arbitrary unitary matrix $\hat{U}$ can be presented in the form

$$\hat{U} = \begin{pmatrix} \mu_0 + \mathrm{i}\mu_1 & \mu_2 + \mathrm{i}\mu_3 \\ -\mu_2 + \mathrm{i}\mu_3 & \mu_0 - \mathrm{i}\mu_1 \end{pmatrix}, \tag{A2}$$

where $|\mu_0|^2 + |\mu_1|^2 + |\mu_2|^2 + |\mu_3|^2 = 1$. This expression can be rewritten in terms of the Pauli matrices

$$\hat{\sigma}_1 = \begin{pmatrix} \mathrm{i} & 0 \\ 0 & -\mathrm{i} \end{pmatrix}, \quad \hat{\sigma}_2 = \begin{pmatrix} 0 & 1 \\ -1 & 0 \end{pmatrix}, \quad \hat{\sigma}_3 = \begin{pmatrix} 0 & \mathrm{i} \\ \mathrm{i} & 0 \end{pmatrix}$$

and will then have the form

$$\hat{U} = \mu_0\sigma_0 + \mu_1\sigma_1 + \mu_2\sigma_2 + \mu_3\sigma_3. \tag{A3}$$

The matrices $\hat{\sigma}_i$ ($i = 1, 2, 3$) satisfy the following relations:

$$\hat{\sigma}_i^2 = -\hat{\sigma}_0, \quad \hat{\sigma}_i\hat{\sigma}_j = -\hat{\sigma}_i\hat{\sigma}_j = \hat{\sigma}_k, \tag{A4a}$$

where the subscripts i, j and k satisfy the cyclic permutation condition.

The algebra of 2×2 complex matrices is isomorphous to the algebra of quaternions, i.e., hypercomplex numbers with three imaginary units I, J and K satisfying the following relations analogous to (A.4a):

$$\mathrm{I}^2 = \mathrm{J}^2 = \mathrm{K}^2 = -1; \quad \mathrm{IJ} = -\mathrm{JI} = \mathrm{K}, \quad \mathrm{JK} = -\mathrm{KJ} = \mathrm{I}, \tag{A4b}$$
$$\mathrm{KI} = -\mathrm{IK} = \mathrm{J}.$$

Thus, carrying out the substitution

$$\hat{\sigma}_0 \to 1, \ \hat{\sigma}_1 \to \mathrm{I}, \ \hat{\sigma}_2 \to \mathrm{J}, \ \hat{\sigma}_3 \to \mathrm{K}, \tag{A5}$$

we can treat the matrix $\hat{U}$ as a quaternion $\tilde{U} = \mu_0 + \mu_1\mathrm{I} + \mu_2\mathrm{J} + \mu_3\mathrm{K}$. Each quaternion $\tilde{U}$ has a conjugate quaternion $\tilde{U}^* = \bar{\mu}_0 - \bar{\mu}_1\mathrm{I} - \bar{\mu}_2\mathrm{J} - \bar{\mu}_3\mathrm{K}$ (the bar indicates complex conjugation) and a norm $\tilde{U}\tilde{U}^* = \tilde{U}^*\tilde{U} = |\mu_0|^2 + |\mu_1|^2 + |\mu_2|^2 + |\mu_3|^2$. Unitary matrices correspond to quaternions with a unit norm associated with them.

Let us define the quaternion $\langle\tilde{G}_0\rangle$ corresponding to the matrix $\langle\hat{G}_0\rangle$. The factorised distribution function (4) allows a successive averaging of the expression (14):

$$\langle\tilde{G}_0\rangle = \langle\tilde{Q}_N^*\langle\tilde{Q}_{N-1}^*\langle\ldots\langle\tilde{Q}_2^*\langle\tilde{Q}_1^*\tilde{M}\tilde{Q}_1\rangle|_1\tilde{Q}_2\rangle|_2\ldots\rangle|_{N-2}$$
$$\times\tilde{Q}_{N-1}\rangle|_{N-1}\tilde{Q}_N\rangle|_N,$$

where

$$\tilde{M} = (1 + \mathrm{iI}\cos 2\varphi - \mathrm{iK}\sin 2\varphi)/2;$$

$$\tilde{Q}_k = \tilde{Q}(\delta_k, \theta_k) = \cos(\delta_k/2) + \mathrm{I}\sin(\delta_k/2)\cos 2\theta_k \tag{A6}$$
$$-\mathrm{K}\sin(\delta_k/2)\sin 2\theta_k; \quad \tilde{Q}^*(\delta_k, \theta_k) = \tilde{Q}(-\delta_k, \theta_k);$$

and $\langle\ldots\rangle|_k$ indicates averaging over the kth set of variables:

$$\langle\ldots\rangle|_k = \int_0^\infty \mathrm{d}l_{gk}\int_{-\pi}^{\pi}\mathrm{d}\alpha_k\int_{-\pi/2}^{\pi/2}\mathrm{d}\beta_k$$
$$\times\int_{-\pi}^{\pi}\mathrm{d}\Phi_k\{(\ldots)f(l_{g_k}, \alpha_k, \beta_k, \Phi_k)\}. \tag{A7}$$

Right and left multiplication of each quaternion $\tilde{G}_0^{(k)} \equiv \tilde{Q}_k^*\ldots\tilde{Q}_2^*\tilde{Q}_1^*\tilde{M}\tilde{Q}_1\tilde{Q}_2\ldots\tilde{Q}_k = x_k + \mathrm{I}y_k + \mathrm{J}z_k + \mathrm{K}w_k$ (where x_k, y_k, z_k and w_k are the corresponding coefficients of the quaternion $\tilde{G}_0^{(k)}$) by $\tilde{Q}_{k+1}$ and $\tilde{Q}_{k+1}^*$ leads to the transformation of real and imaginary parts respectively ($\tilde{G}_0^{k+1} = x_{k+1} + \mathrm{I}y_{k+1} + \mathrm{J}z_{k+1} + \mathrm{K}w_{k+1}$), which can be written in the form

$$x_{k+1} = x_k, \quad \begin{pmatrix} y_{k+1} \\ z_{k+1} \\ w_{k+1} \end{pmatrix} = \hat{S}(\delta_{k+1}, \theta_{k+1})\begin{pmatrix} y_k \\ z_k \\ w_k \end{pmatrix},$$

where

$$\hat{S}(\delta, \theta) =$$

$$\begin{pmatrix} 1 - 2\sin^2\frac{\delta}{2}\sin^2 2\theta & -\sin\delta\sin 2\theta & -\sin^2\frac{\delta}{2}\sin 4\theta \\ \sin\delta\sin 2\theta & \cos\delta & \sin\delta\cos 2\theta \\ -\sin^2\frac{\delta}{2}\sin 4\theta & -\sin\delta\cos 2\theta & 1 - 2\sin^2\frac{\delta}{2}\cos^2 2\theta \end{pmatrix}; \tag{A8}$$

$$x_0 = 1/2; \ y_0 = \mathrm{i}\frac{\cos 2\varphi}{2}; \ z_0 = 0; \ w_0 = -\mathrm{i}\frac{\sin 2\varphi}{2}. \tag{A9}$$

Note that each optical element which is described by a normalised quaternion $\tilde{U}$ has a 3×3 unitary matrix, which defines a transformation of the type (A.8), corresponding to it. If the matrix $\hat{U}$ is not unitary, this transformation is assigned by a 4×4 matrix.

For a very large value of N (when $\varepsilon = p/N \ll 1$) $\sin\delta = \delta + \mathrm{O}(\varepsilon^3)$ [see Eqn (1)] and the matrix $\hat{S}$ can be written in the form $\hat{S}(\delta, \theta) = 1 + \varepsilon\eta\hat{\Sigma}(\delta, \theta) + \frac{1}{2}\varepsilon^2\eta^2\hat{\Sigma}^2(\delta, \theta) + \mathrm{O}(\varepsilon^3)$, where

$$\eta = \frac{l_g}{\langle l_g\rangle}; \quad \hat{\Sigma}(\delta, \theta) = \begin{pmatrix} 0 & \tilde{b} & 0 \\ -\tilde{b} & 0 & -\tilde{a} \\ 0 & \tilde{a} & 0 \end{pmatrix}. \tag{A10}$$

We shall restrict ourselves to terms of the order of ε^2. Going over from the quaternion $\langle\tilde{G}_0\rangle$ to the matrix $\langle\hat{G}_0\rangle$ and substituting it into (8), we obtain

$$\langle\Gamma_0\rangle = x_0 + \mathrm{i}y_N\cos 2\varphi - \mathrm{i}w_N\sin 2\varphi, \tag{A11}$$

where

$$\begin{pmatrix} y_N \\ z_N \\ w_N \end{pmatrix} = \hat{S}_\mathrm{t}\begin{pmatrix} y_0 \\ z_0 \\ w_0 \end{pmatrix}; \tag{A12}$$

$$\hat{S}_\mathrm{t} = \langle\hat{S}\rangle^N; \quad \langle\hat{S}\rangle = 1 + \varepsilon\begin{pmatrix} 0 & 0 & 0 \\ 0 & 0 & -a \\ 0 & a & 0 \end{pmatrix}$$
$$-\frac{1}{2}\varepsilon\begin{pmatrix} B & 0 & 0 \\ 0 & A^2 + a^2 + B & 0 \\ 0 & 0 & A + a^2 \end{pmatrix}.$$

Here we have used the notation adopted in (21). Raising to the Nth power and substituting it in (A.12), we can determine y_N and w_N. Substituting these into (A.11), we obtain the local depolarisation

$$\langle\Gamma_0\rangle = \sin^2 2\varphi\sin^2\frac{\Delta}{2} + \frac{p^2}{4N}\left[B\cos^2 2\varphi + \left(A + \frac{1}{2}B\right)\times\right.$$

$$\times \sin^2 2\varphi \cos \Delta \Big] - \frac{p}{8N} \frac{B}{a} \sin^2 2\varphi \sin \Delta. \quad \text{(A13)}$$

Calculation of $\langle \Gamma_{1-3} \rangle$ for schemes with compensation (Figs 2b–d) is performed similarly. In contrast to the preceding problem, the matrix $\hat{S}_t$ for scheme I is transformed into the matrix $\hat{S}_{t1} = \langle \hat{S}(\Delta) \rangle^N \langle \hat{S}(-\Delta) \rangle^N$. The calculation gives

$$\langle \Gamma_1 \rangle = \frac{p^2}{2N} \left[B \cos^2 2\varphi + \left(A + \frac{1}{2} B \right) \sin^2 2\varphi \right]$$

$$- \frac{p}{8N} \frac{B}{a} \sin^2 2\varphi \sin 2\Delta. \quad \text{(A14)}$$

In scheme II, a uniaxial crystal has the following matrix corresponding to it:

$$\hat{S}_c = \hat{S}(-\Delta, 0) = \begin{pmatrix} 1 & 0 & 0 \\ 0 & \cos \Delta & -\sin \Delta \\ 0 & \sin \Delta & \cos \Delta \end{pmatrix},$$

hence $\hat{S}_{t2} = \hat{S}_c \langle \hat{S} \rangle^N$, which gives

$$\langle \Gamma_2 \rangle = \frac{\langle \Gamma_1 \rangle}{2}. \quad \text{(A15)}$$

For scheme III, we have $\hat{S}_{t3} = \langle \hat{S} \rangle^N \hat{S}_{\lambda/2} \langle \hat{S} \rangle^N$, where

$$\hat{S}_{\lambda/2} = \hat{S}(\pi, -\varphi) = \begin{pmatrix} \cos 4\varphi & 0 & -\sin 4\varphi \\ 0 & -1 & 0 \\ -\sin 4\varphi & 0 & \cos 4\varphi \end{pmatrix},$$

and hence

$$\langle \Gamma_3 \rangle = \sin^2 4\varphi \sin^4(\Delta/2) - \frac{p}{8N} \frac{B}{a}$$

$$\times (\sin^2 2\varphi \cos 4\varphi \sin 2\Delta - \sin^2 4\varphi \sin \Delta)$$

$$+ \frac{p^2}{2N} \left[B \cos^2 2\varphi \cos 4\varphi + \left(A + \frac{1}{2} B \right) \sin^2 2\varphi \right.$$

$$\left. \times (1 - 2\cos^2 2\varphi \cos^2 \Delta) + \left(\frac{1}{2} A + \frac{3}{4} B \right) \sin^2 4\varphi \cos \Delta \right]. \quad \text{(A16)}$$

Relations (18)–(20) for γ_{0-3} are obtained by integrating the expressions (A.13)–(A.16) with respect to r and φ.

References

1. Taira T., Ikesue A., Yoshida K. *OSA TOPS on Advanced Solid-State Lasers*, **19**, 430 (1998).
2. Shoji I., Sato Y., Kurimura S., Lupei V., Taira T., Ikesue A., Yoshida K. *Opt. Lett.*, **27**, 234 (2002).
3. Shoji I., Kurimura S., Sato Y., Taira T., Ikesue A., Yoshida K. *Appl. Phys. Lett.*, **77**, 939 (2000).
4. Lu J., Murai T., Takaichi K., Uematsu T., Misawa K., Prabhu M., Xu J., Ueda K., Yagi H., Yanagitani T., Kaminskii A.A., Kudryashov A. *Appl. Phys. Lett.*, **78**, 3586 (2001).
5. Lu J., Prabhu M., Song J., Li C., Xu J., Ueda K., Kaminskii A.A., Yagi H., Yanagitani T. *Appl. Phys. B*, **71**, 469 (2000).
6. Khazanov E.A. *Opt. Lett.*, **27**, 716 (2002).
7. Lu J.R., Lu J.H., Murai T., Takaichi K., Uematsu T., Ueda K., Yagi H., Yanagitani T., Kaminskii A.A. *Jpn. J. Appl. Phys.*, Pt. 2, **40**, L1277 (2001).
8. Ainola L., Aben H. *J. Opt. Soc. Am. A*, **18**, 2164 (2001).
9. Richartz M., Hsu H.-Y. *J. Opt. Soc. Am.*, **39**, 136 (1949).
10. Khazanov E., Andreev N., Palashov O., Poteomkin A., Sergeev A., Mehl O., Reitze D. *Appl. Opt.*, **41**, 483 (2002).
11. Landau L.D., Lifshitz E.M. *Mekhanika* (Mechanics) (Moscow: Nauka, 1973).
12. Mezenov A.V., Soms L.N., Stepanov A.I. *Termooptika tverdotel'nykh lazerov* (Thermo-optics of Solid State Lasers) (Leningrad: Mashinostroeniye, 1986).
13. Scott W.C., de Wit M. *Appl. Phys. Lett.*, **18**, 3 (1971).
14. Gelikonov V.M., Gusovskii D.D., Leonov V.I., Novikov M.A. *Pis'ma Zh. Tekh. Fiz.*, **13**, 775 (1987).
15. Khazanov E., Poteomkin A., Katin E. *J. Opt. Soc. Am. B*, **19**, 667 (2002).
16. Clarkson W.A., Felgate N.S., Hanna D.C. *Opt. Lett.*, **24**, 820 (1999).
17. Malykin G.B., Pozdnyakova V.I., Shereshevskii I.A. *Izv. Vyssh. Uchebn. Zaved. Ser. Radiofiz.*, **43**, 976 (2000).
18. Rytov S.M., Kravtsov Yu.A., Tatarskii V.I. *Vvedenie v statisticheskuyu radiofiizku* (Introduction to Statistical Radiophysics) (Moscow: Nauka, 1978) Vol. II.
19. Takaichi K., Lu J.R., Murai T., Uematsu T., Shirakawa A., Ueda K., Yagi H., Yanagitani T., Kaminskii A.A. *Jpn. J. Appl. Phys. Pt 2*, **41**, L96 (2002).
20. Ikesue A. *Private communication* (2002).